metals

MDPI

Review

Review of Microstructures and Properties of Zinc Alloys

Annalisa Pola [1,*], Marialaura Tocci [1] and Frank E. Goodwin [2]

[1] Department of Mechanical and Industrial Engineering, University of Brescia, Via Branze, 38-25123 Brescia, Italy; marialaura.tocci@unibs.it

[2] International Zinc Association, 2530 Meridian Parkway, Durham, NC 27713, USA; fgoodwin@zinc.org

* Correspondence: annalisa.pola@unibs.it; Tel.: +39-030-371-5576

Received: 15 January 2020; Accepted: 11 February 2020; Published: 14 February 2020

Abstract: According to market data, about 15% of world zinc consumption is devoted to the production of zinc-base alloys that are used for manufacturing automotive parts, electronic/electrical systems and also, water taps and sanitary fittings, household articles, fashion goods, etc. These alloys are characterized by low melting points and high fluidity that make them suitable for foundry applications. Typically, they are processed by hot chamber high-pressure die-casting where can be cast to thicknesses as low as 0.13 mm. The die-cast zinc alloys possess an attractive combination of mechanical properties, permitting them to be applied in a wide variety of functional applications. However, depending on the alloying elements and purposes, some zinc alloys can be processed also by cold chamber die-casting, gravity, or sand casting as well as spin casting and slush casting. In this paper, a detailed overview of the current knowledge in the relationships between processing, microstructure and mechanical properties of zinc-base alloys will be described. In detail, the evolution of the microstructure, the dimensional stability and aging phenomena are described. Furthermore, a thorough discussion on mechanical properties, as such as hardness, tensile, creep, and wear properties of zinc-base alloys is presented.

Keywords: zinc alloys; zamak; ZA; aging

1. Introduction

Zinc is the fourth metal in the world, after iron, aluminum and copper. In 2018, the global zinc supply increased up to 13.4 Mt with a global demand of 13.77 Mt [1]. Significant amounts of zinc are also recycled and secondary zinc production is estimated in the order of 20–40% of global consumption [2]. However, because of the strict limitation on impurities in die-casting composition standards, almost all zinc die-casting alloys are prepared from primary zinc production.

In general, about a half of the consumed zinc finds its application in the galvanizing steel, preventing corrosion [3]. Other important applications involve the use of zinc for other coatings, or as alloying element in brasses, bronzes, aluminum, and magnesium alloys. Zinc is exploited also as oxide in chemical, pharmaceutical, cosmetics, paint, rubber, and agricultural industries. Recently, zinc has been investigated as a promising alternative to iron and magnesium as new biodegradable metal [4]. However, about 15% of world zinc is used as base metal for the production of zinc-base alloys [5]. Some of them are available on the market as wrought alloys, in the form of flat-rolled, wire-drawn, and extruded and forged products. They are applied in the construction field for the production of roofing, downspouts, gutters, flashlight reflectors, parts for lamps, etc. Lately, a new zinc alloy for extrusion and forging has been also developed [6].

Zinc-base alloys offer a series of properties that makes them particularly attractive for die-casting manufacturing and, in general, for foundry technologies. In fact, they are characterized by a low

melting temperature, resulting in low energy consumption and long die life, combined with high fluidity, that helps in filling complex mold cavities and very thin sections, typically as low as 0.75 mm or even down to 0.13 mm [7]. They show good mechanical properties, including equivalent, or often better, bearing and wear properties than conventional Cu alloys [8,9]. Additionally, they offer good finishing and ability to be easily plated, making them more resistant to corrosion and wear and improving their aesthetic appearance. On the contrary, they suffer from reduction in performance above 80–90 °C [10] and/or after long exposure at room temperature (aging) [11]. For these reasons, they are mainly used for small non-structural components in many fields as such as automotive, hardware, electric/electronic devices, clothes, toys, sports, ornaments, etc. For instance, parts like safety belt blocks, locking mechanisms, wiper motor housings, cylinder locks, some electronic connectors, handles, tap systems, zippers, belt buckles, spring adjuster in bikes, costume jewelry, appliances, etc. are made from zinc-base alloys (Figure 1).

Figure 1. Examples of cast zinc-base alloys products.

The main limitations to wider usage of zinc alloys relate to their high density and loss of mechanical properties with increased temperature and time [12].

2. Alloys and Manufacturing Technologies

Nowadays there are more than 25 alloys used in foundry and the most commercially relevant are specified in international standards (e.g., EN 12844) [5]. In Table 1, the chemical compositions of the most frequently applied alloys are reported, according to the ASTM B86 standard [13].

Table 1. Chemical composition (wt. %) of some zinc-base alloys [13].

Alloy	Al%	Cu%	Mg%	Fe%	Pb%	Cd%	Sn%	Ni%	Cr%	Si%	Zn%
Zamak 2 (AC43A)	3.7–4.3	2.6–3.3	0.02–0.06	<0.05	<0.005	<0.004	<0.002	-	-	-	rest.
Zamak 3 (AC40A)	3.7–4.3	<0.1	0.02–0.06	<0.05	<0.005	<0.004	<0.002	<0.02	<0.02	<0.035	rest.
Zamak 5 (AC41A)	3.7–4.3	0.7–1.2	0.02–0.06	<0.05	<0.005	<0.004	<0.002	<0.02	<0.02	<0.035	rest.
Zamak 7	3.7–4.3	<0.1	0.005–0.02	<0.05	<0.003	<0.002	<0.001	0.005–0.02	<0.02	<0.035	rest.
ZA8	8.0–8.8	0.8–1.3	0.01–0.03	<0.075	<0.006	<0.006	<0.003	<0.01	<0.01	-	rest.
ZA12	10.5–11.5	0.5–1.2	0.01–0.03	<0.075	<0.006	<0.006	<0.003	<0.01	<0.01	-	rest.
ZA27	25–28	2–2.5	0.01–0.02	<0.075	<0.006	<0.006	<0.003	<0.01	<0.01	-	rest.
ACuZinc 5	2.5–3.3	5.0–6.0	0.02–0.05	<0.075	0.005	<0.004	<0.003	<0.01	-	-	rest.
ACuZinc 10	2.5–3.3	10–11	0.02–0.05	<0.075	0.005	<0.004	<0.003	<0.01	-	-	rest.
ALZEN 305	30	5	0.01–0.02	-	-	-	-	-	-	-	rest.
ALZEN 501	50	1	0.01–0.02	-	-	-	-	-	-	-	rest.
ZEP®	14–16	0.8–1.2	0.025–0.035	<0.03	<0.0003	<0.0001	<0.0001	-	-	<0.02	rest.

Other alloys with their corresponding compositions and brand names can be found in the literature [14].

Aluminum has an appreciable solubility in zinc. It is added because it creates a eutectic phase at 381 °C and 6% of Al (Figure 2) that increases the alloy fluidity and reduces melting temperature,

making the alloys particularly suitable for foundry. It also enhances mechanical properties [5,10]. Moreover, the eutectoid alloy has been found to exhibit exceptional elongation at room temperature, i.e., superplastic behavior [15].

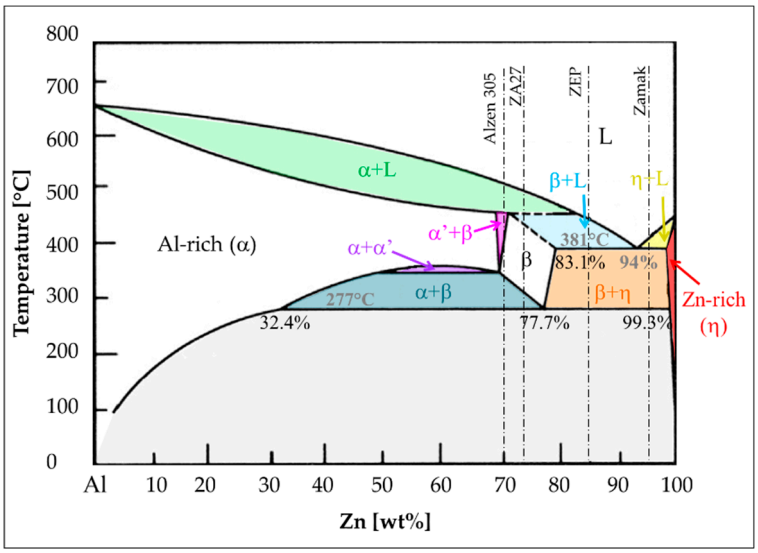

Figure 2. Zinc-Al phase diagram.

Copper is added to increase the alloy performance in terms of tensile strength, hardness and wear resistance, as well as creep behavior [16]. Usually, a small amount of Mg is also present to inhibit inter-granular corrosion [17], even if in modern practice its need is very limited because of the high purity of Zn [11].

Depending on the amount of alloying elements, zinc alloys usually available on the market can be manufactured by means of different processes: hot chamber die-casting, cold chamber die-casting, gravity and sand casting, as well as spin casting and slush casting.

Die-casting involves the injection of the molten metal into a permanent die, under high pressure and high speed. This allows to obtain near-net shape castings, characterized by thin sections, tight dimensional tolerances, smooth surfaces, high production rates, etc. In particular, in hot-chamber process the injection system (including a pump that feeds a heated channel called the gooseneck) is submerged into the crucible containing the molten alloy. On the contrary, in cold-chamber die-casting the furnace is separate from the casting machine and the liquid metal is transferred into the injection system (shot sleeve) by a ladle [18]. About the 90–95% of zinc alloys are typically processed via hot-chamber die-casting technique thanks to their low melting temperature [5]. When the amount of alloying elements increases, like in the case of ZA27 or ACuZinc 10, cold-chamber die-casting is required as a result of the associate increase in their melting temperature and attitude to attack, react with or dissolve the injection system.

For limited applications also gravity or sand casting are applied, where the metal is poured by gravity in a mold made in steel or refractory material respectively. Typical components produced with these technologies are press dies and punches for sheet metal forming or molds for ceramics and rubber using Kirksite (i.e., Zamak 2) [19].

Spin casting exploits a centrifugal force to fill a mold made of rubber. This technique is particularly suitable for low melting alloys, like some zinc-base ones, resulting in a cheap and fast method for the production of small parts, short run and prototypes for fashion industry, miniature models, fishing lures, etc.

For the production of hollow products, like some table lamp bases, also slush casting is used [20]. It consists in pouring the liquid metal into the mold, allowing the solidification of a shell on the wall of the mold. The remaining liquid in the core is then poured out, leaving the hollow shell characterized by

a good surface. For this casting technology, zinc alloys with very high fluidity and narrow solidification range are needed, like those containing around 5–6% of Al and 1% of Cu [5,20].

It has to be noticed that all the above-mentioned Zn alloys do not usually undergo cold working or heat treatment to improve mechanical properties because of the risk of crack formation during cold working (low plasticity) and because of the limited effectiveness of age hardening [11]. Therefore, except some surface finishing, they are normally used in the as-cast condition. It follows that the quality of the part and their microstructure plays a major role in defining component performances.

3. Microstructures

As already reported, zinc casting alloys always contain aluminum as main alloying element. Hence, in agreement with Zn-Al phase diagram (Figure 2), they could be distinguished in three categories: hypoeutectic (e.g., Zamak), hypereutectic (e.g., ZA12, ZEP), and hypereutectoid alloys (e.g., ZA27, Alzen 305).

The hypoeutectic alloys are the most widely used in industrial applications, as they correspond to the hot-camber die-casting alloys, commercially known as Zamak. The hyper-eutectic/eutectoid ones are more devoted to cold chamber process or gravity and sand casting, covering a more restricted market. The corresponding microstructures are therefore different, depending also on the specific cooling rate related to the foundry process.

In Figure 3a, the metallographic analysis of a Zamak 5 die-cast part after Nital 2% etching is reported as an example of the hypoeutectic alloys. Primary Zn-rich η dendrites (white) surrounded by the η + β eutectic can be distinguished. The microstructure at higher magnification (Figure 3b) reveals that the eutectoid consists of platelets of Al-rich phase dispersed in Zn-rich one. As shown by the scanning electron microscope with energy dispersive spectroscopy microanalysis (SEM-EDS), Cu is mainly retained in solid solution in the primary phase. In case of alloy containing Cu in percentage higher than 2%, like for instance in Zamak 2, also Cu-rich ε-phase ($CuZn_4$) can be easily found [21].

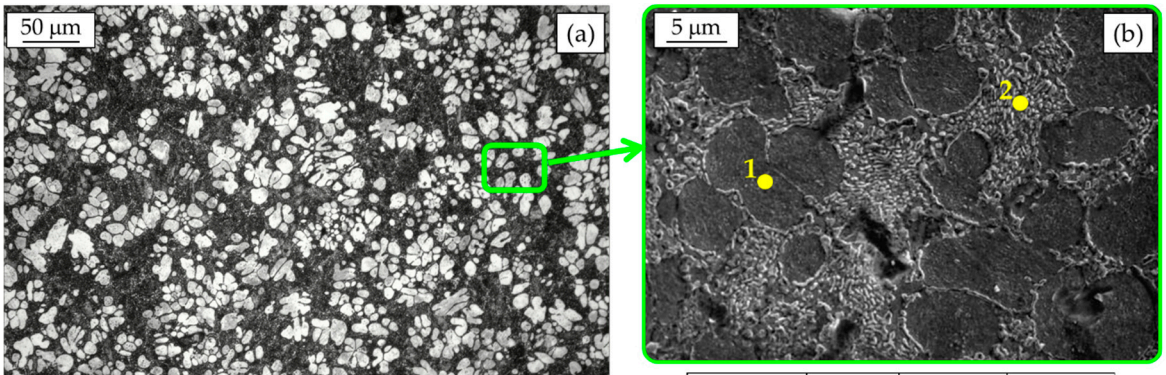

Spectrum	Al wt%	Cu wt%	Zn wt%
1	1.29	1.53	97.19
2	11.79	0.59	87.62

Figure 3. Hypoeutectic Zamak 5 microstructure (**a**) and SEM-EDS analysis (**b**).

In Figure 4a, the microstructure of an as-cast ZEP alloy can be observed. Primary Al-rich β dendrites surrounded by the divorced eutectic η + β can be clearly seen. Dendrites appear slightly larger than in the previous case due to the different foundry process, i.e., different cooling rates during solidification. According to the phase diagram, when the eutectoid temperature is reached, the β phase decomposes in a very fine α+η mixture, as noticeable at higher magnification (Figure 4b). In particular, the SEM-EDS analysis highlights the different morphology and composition of β after eutectoid decomposition, which is characterized by a lamellar microstructure of α + η with a chemical composition similar to the eutectic phase formed from solidification (spectrum 2 of Figure 4b) [22]. The surrounding coarser globular microstructure of α + η (spectrum 3 of Figure 4b) corresponds

to the divorced β eutectic and it is characterized by a chemical composition close to the eutectoid one (i.e., Al = 21.77%). A more detailed explanation of this solid-state transformation can be found in the literature [22].

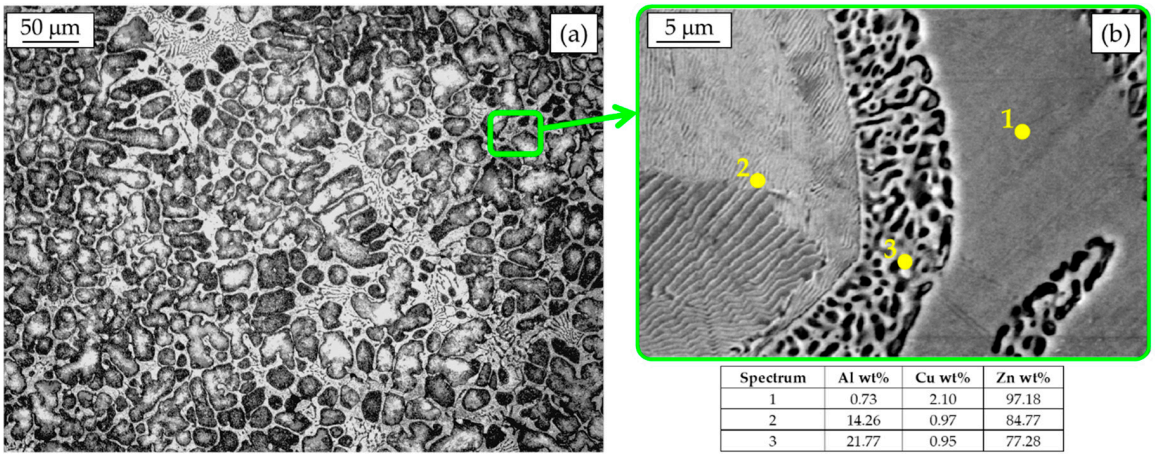

Spectrum	Al wt%	Cu wt%	Zn wt%
1	0.73	2.10	97.18
2	14.26	0.97	84.77
3	21.77	0.95	77.28

Figure 4. Hyper-eutectic ZEP microstructure (**a**) and SEM-EDS analysis (**b**).

In Figure 5, the microstructures of gravity cast hyper-eutectoid alloys such as the ZA27 or Alzen 305 are reported. Primary Al-rich β-dendrites can be observed with inter-dendritic films and, somewhere, pools of eutectic, resulting from the solidification condition [22]. The dissimilar color moving from the core to the boundary of the dendrites arms is related to the different Al concentration, in details lower at the borders and higher in the center [23].

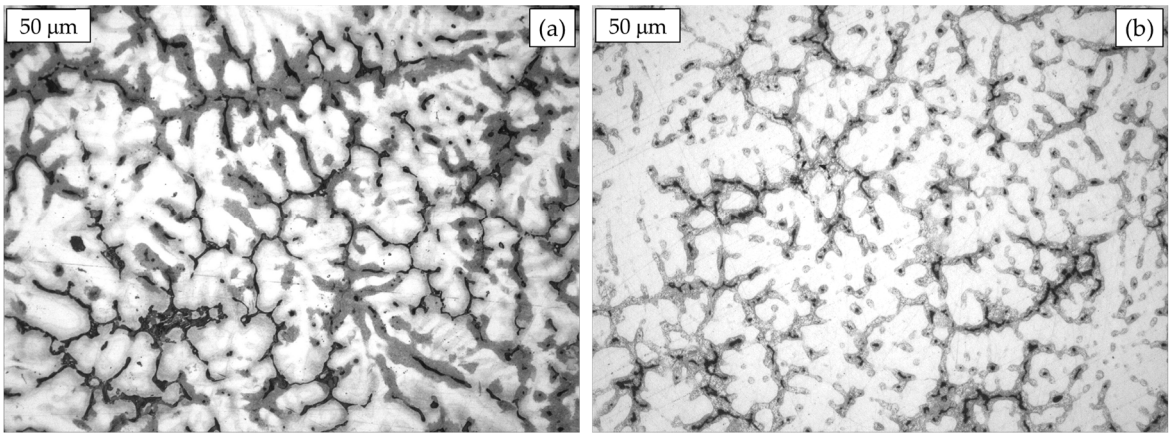

Figure 5. Hyper-eutectoid ZA27 (**a**) and Alzen 305 microstructures (**b**).

4. Performance of Zinc Alloys

Notwithstanding that zinc alloys are used for functional, decorative and non-structural products, the knowledge about their performance is fundamental for their proper application under different service conditions. Hence, in the last decades, several studies have been focused on the investigation of mechanical, technological and electro-chemical properties of parts fabricated in zinc alloys, sometimes in comparison with other non-ferrous metals (mainly brass).

4.1. Tensile Properties and Hardness

The mechanical properties of zinc alloys mainly depend at on two factors: the casting conditions and the alloy chemical composition.

Concerning the first point, each foundry process is characterized by specific solidification/cooling rates that are responsible of the final part microstructure. In particular, high pressure die-casting (D) is expected to promote rapid solidification and cooling, giving rise to a fine microstructure, meanwhile sand (S) or gravity (G) casting are characterized by slower cooling rates which determines a coarser microstructure [24]. As a result, a sound die-cast part should show higher mechanical properties than a gravity or sand cast one. This can be clearly noticed when comparing the data available in the literature and summarized in Table 2.

Table 2. Mechanical properties of some zinc-base alloys [25–27].

Alloy	Tensile Strength (MPa)	Yield Strength (MPa)	E%
Zamak 2 (D)	358	-	7
Zamak 3 (D)	283	-	10
Zamak 5 (D)	331	-	7
Zamak 7 (D)	283	-	13
ZA-8 (S)	248–276	200	1–2
ZA-8 (G)	221–255	207	1–2
ZA-8 (D)	372	290	6–10
ZA-12 (S)	276–317	207	1–3
ZA-12 (G)	310–345	207	1–3
ZA-12 (D)	400	317	4–7
ZA-27 (S)	400–440	365	3–6
ZA-27 (G)	421–427	365	1
ZA-27 (D)	421	365	1–3
ACuZinc 5 (D)	407	338	0.4
ACuZinc 5 (G)	297	-	5

The influence of conventional alloying elements as Al and Cu on mechanical properties has been widely discussed in the literature [10,28–32]. Liu et al. [28], for instance, focused their attention on binary gravity cast Zn-Al alloys with low aluminum percentage (hypo-eutectic) after annealing, finding a certain relationship between the amount of Al and the mechanical properties. They showed that hardness, elongation, and yield stress of the Zn-Al alloys increase because of the grain-refinement, solid-solution, and secondary phase (skeleton) strengthening mechanisms induced by the alloying element addition. Hekimoğlu et al. [29] investigated the effect of higher Al content (5–25%) on G-cast Zn-base alloys, showing that hardness and strength increase with the Al content, meanwhile the impact energy decreases. They ascribed these results to both the size and the volume fraction of the relatively hard β dendrites, which increase with Al, combined with the solid solubility of Zn in Al-rich phase. Additionally, they observed a sharp increase in the total percentage elongation by increasing Al content up to 10%, as a consequence of the decrease in eutectic mixture, the transformation of pro-eutectic β dendrites into eutectoid α + η phases and the formation of α particles in inter-dendritic regions resulting from the decomposition of eutectic β phase [29,32]. However, above this percentage, the trend reverses because of the different amount of phases present in the microstructure [29]. Similar findings have been reported in [30], where the effect of Al addition in the range of 15–50 wt. % was analyzed, using the same casting technology (G) for the samples production. Again, a sort of relationship between Al percentage and performance was detected, as shown in Figure 6a for what concerns the hardness. These results are in agreement with the data from Abou El-khair et al. [10], who analyzed also the effect of the temperature on mechanical properties. Their findings further confirm the increase in ultimate and yield strength with the Al content. Additionally, they showed the same trend also at high temperature although with lower values, as summarized in Figure 6b.

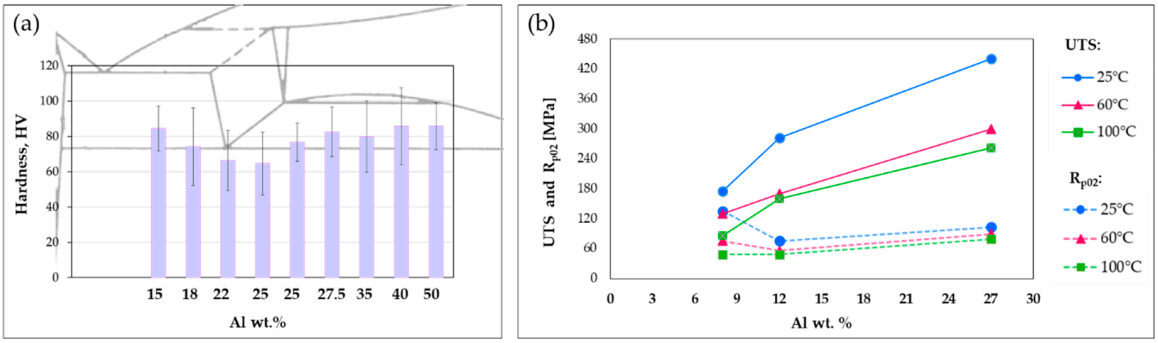

Figure 6. Effect of Al addition on Zn-Al alloys (**a**) hardness (based on data from [30]) and (**b**) tensile and yield strength (based on data from [10]).

It must be emphasized that many of the cited papers report differing values of mechanical properties for the same alloys. This can be easily explained considering the different samples sizes and casting parameters (mold temperature, runner and gating system, etc.), i.e., different solidification and cooling rates, which result in dissimilar microstructure and casting defects distribution. However, the same trend with the Al addition is well documented.

Concerning the influence of Cu on Zn-Al alloys, there is a general agreement about its effectiveness in increasing both hardness and tensile strength due to the solid solution strengthening mechanism [21,30,31]. However, when copper exceeds a certain level (around 2 wt. %), the copper-rich ε ($CuZn_4$) phase forms in the inter-dendritic region of the ternary Zn-Al-Cu alloys, resulting in an increase in the cracking tendency and a reduction in the impact energy of the alloys, meanwhile the hardness almost increases continuously with copper.

Different authors also investigated the effect of small percentages of other elements, those not typically used in Zn alloys, such as Mn, Si, Li, Y, Ce, Ti, B, Sr, Ni, etc. [21,33–38]. These elements appear to increase the mechanical properties, like hardness, tensile or impact strengths. However, they all have very limited solubility in the traditional Zn alloys and until now have not gone further than basic research studies.

4.2. *Effect of Aging*

Zinc alloys experience a remarkable reduction of mechanical properties with time at room temperature. This drop in performance, called aging, is well documented in the literature [12,39,40]. After one year of maintenance at room temperature, Zn alloys can experience a reduction in tensile strength in the order of 5–15%, depending on the alloy composition and specimen thickness (i.e., cooling rate/microstructure) [17,40].

Susceptibility to this phenomenon results from the non-equilibrium solidification and cooling conditions typical of cast products, which induce subsequent solid-state transformations towards more stable configurations. These reactions take place extremely slowly at room temperature and at higher rates as the temperature is increased [8]. In fact, Zn alloys age already at low temperature as diffusion at room temperature is rather high due to the low melting point of zinc [41].

Very thin castings, having a fine microstructure due to the fast cooling, are characterized by the smallest diffusion distances. It follows that the reduction in tensile strength with time is the fastest for the thinnest castings. Moreover, depending on the alloy chemical composition and casting thickness, a maximum strength can be detected after some days of natural ageing, which is related to the growth and dissolution of copper-rich ε phase [41].

To stabilize the properties of zinc alloys, artificial aging treatments at 65–105 °C have been frequently proposed [12,39–41]. Artificial aging for 24 h at 85 °C is shown to lead only to a partial decrease in performance. In fact, the results in terms of mechanical properties are not comparable to

those after natural aging for one year. Additionally, artificial aging at this temperature does not match the extent of natural aging seen in thin samples because of the longer diffusion distances in thicker ones.

On the contrary, it was demonstrated for some zinc alloys that 24 h aging at 105 °C results almost in the same changes in properties that would take place in one year at room temperature, assessing a consistent relationship between natural and artificial aging. Furthermore, mechanical tests performed maintaining specimens at this temperature for different times showed that the maximum drop in properties occurs in the first 24 h, while they are almost stable for longer soaking times [42].

It has to be noted that some of these reactions are accompanied by volumetric changes, resulting also in a slight but measurable dimensional instability of Zn-Al castings (most of all in those containing Cu). This determines first an expansion or a shrinkage and then an expansion even up to 4% [12,43,44]. This is mainly related to the formation of the metastable Cu-rich ε-phase ($CuZn_4$) with a hexagonal close packed structure that evolves to form the stable (Al_4Cu_3Zn) T′ phase. This is a consequence of the four-phase reaction $\alpha + \varepsilon \rightarrow \eta + T'$ that leads to an increase in volume [43,45].

4.3. Wear and Cavitation Resistance

Wear resistance is particularly important for Zn-base alloys due to the specific application fields of these materials, ranging from fashion and decorative (buckles, chain and belts, zippers, etc.) to automotive industry (small gears, gear racks, pulleys, gearboxes, etc.). In addition, as mentioned above, Zn alloys are often used for bearings production to replace Cu-base alloys.

Therefore, sliding wear behavior of Zn-Al alloys has been widely investigated in scientific literature by means of experimental testing mainly with pin-on-disk [9,46,47] or block-on-disk (ring) [48–50] configurations and in dry or lubricated conditions.

It has to be reminded that wear resistance is not an intrinsic property of the material, as it depends on the considered tribological system and the used test conditions. Therefore, a comparison of the wear behavior of alloys tested under different conditions (i.e., different applied load, sliding distance, with or without lubrication, etc.) is not reliable. However, different authors agree about general findings. A common point is that the microstructural features discussed in Paragraph 3 play a major role in determining wear performance of Zn-Al alloys. Considering for instance those with low Al content, hypo-eutectic Zamak 2 and Zamak 3 alloys were studied in comparison with Zn alloys with higher levels of Cu and/or Al [51,52]. In general, the low hardness of Zamak 3 alloy (due to the primary Zn-rich η-phase) results in higher friction coefficient and wear rate than the other alloys when tested against steel counter-part in dry conditions [51]. On the other hand, Zamak 2 alloy is harder, due to the higher Cu content, but it is reported to exhibit worse wear resistance in comparison with alloys with higher Al content alloys (i.e., ZnAl15Cu1 and ZA27). This is likely due to a limited oxide formation on the wear track, especially in the first stages of the test, as shown as an example in Figure 7. On the contrary, the oxide formed on the wear track of ZnAl15Cu1 (ZEP) and ZA27 alloys seems able to protect the surface from damage. However, also Zamak 2 experiences a pronounced oxidation of the track by increasing the sliding distance (i.e., up to 1000 m) [52]. In all the alloys, scratches aligned with the sliding direction can be seen, as a result of the abrasive wear damage.

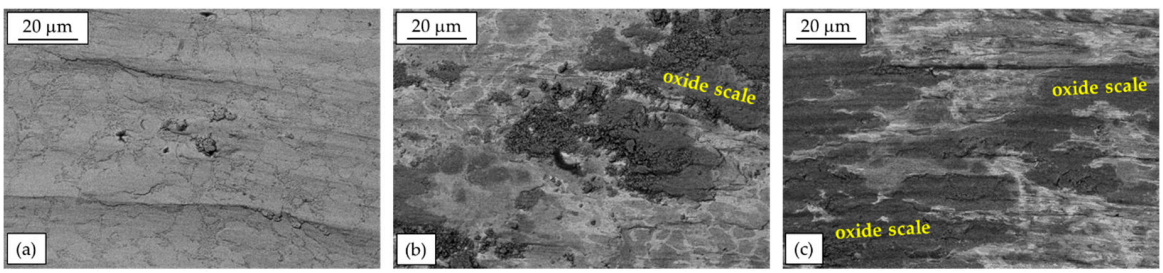

Figure 7. SEM analyses of wear tracks of (**a**) Zamak 2, (**b**) ZnAl15Cu1, and (**c**) ZA27 obtained by pin-on-disk test at 100 m-1 N and 100Cr6 counterpart.

Abou El-khair et al. [10] investigated Zn-Al binary alloys with three Al levels of 8-12-27 wt. %, finding that Al enhances wear resistance especially at high loads (40–100 N) due to the microstructural evolution with increasing Al content. In fact, the α-Al rich phase (present in ZnAl27 alloy) was responsible for an improvement in the load bearing capacity of the alloy in comparison with the other considered compositions (ZnAl8 and ZnAl12).

Possible improvements in wear resistance of Zn alloys with moderate Al content have been investigated, like the addition of Pb, Sn, and Cd for ZA-8 alloy, which was tested by means of pin-on-disk experiments with various sliding speeds and applied loads [47]. It was found that Pb and Cd elements are beneficial for wear resistance, especially at high loads (30–45 N) while Sn lead to poor wear behavior in comparison with the base material (ZA-8). Strengthening of ZA12 alloy by silver addition is reported to be beneficial for wear properties [53].

Because of its significant wear resistance and capability of replacing traditional bronze bearing at low cost [17,54], several studies focused mainly on ZA27 alloy, with or without heat treatment [49,55], and often modified by the addition of other alloying elements [9,56,57]. A key point for its wear performance is represented by the presence of the strengthening α-Al rich phase, even though the alloy suffers from dimensional instability due to the presence of Cu. In this regard, some authors investigated the influence of the addition of Si to Zn-Al alloys as an alternative to Cu [58,59]. It was found that the alloy containing Si exhibited excellent wear resistance in lubricated conditions due to the formation of hard load-bearing Si particles in the Zn-Al matrix. Furthermore, Zn-Al-Si alloy showed an improved dimensional stability. This was confirmed also by another research, in which tests were performed in lubricated condition and for high load and intermediate speed [46]. In addition, Prasad et al. [9] studied wear resistance in dry condition for ZA27 alloy containing Si and Ni and found that Si particles and Ni-containing intermetallic are responsible for a slightly higher crack sensitive behavior of the alloy in comparison with the base one, still guaranteeing better wear resistance than bronzes. Similar results were found for ZA27 alloy modified with Sb [57] or with graphite particles, alumina, zirconia particles, and fly ashes in particular to improve the properties at high temperature [60–63].

Analogous findings were reported also in other studies concerning the dry sliding wear resistance of Zn-Al alloys also with higher Al content. In fact, Pürçek at al. [50] found that ZnAl40Cu2Si1 alloy showed the best wear resistance not only in comparison with bronze but also with ZA27 alloy (tested with and without Si addition).

However, concerning Al-rich Zn alloys, it was documented that an increase in Al content up to 40 and 48 wt. % is not positive for wear resistance [64]. In fact, for these alloys, the higher strength and load bearing capacity of α-phase as compared to η-phase is not sufficient to guarantee good wear performances since these alloys are often characterized by a significant porosity level due to the wide solidification range related to the high Al content. Only for very high load (1000 N), the ZA48 alloy exhibited similar wear rate to ZA27 alloy. Some authors mentioned that for these compositions the η-phase can act as a solid lubricant during sliding wear [50,65].

The role of Cu was systematically investigated for ZnAl27 and ZnAl40 alloys in [31,66]. It is reported that Cu is beneficial for wear resistance up to 2 wt. %, while for higher content no significant improvement in material performance can be appreciated. This is attributed to the α-phase solid-solution hardening effect of Cu up to 2 wt. %, while other phases form if this level of Cu is exceeded, resulting in a decrease of material properties. Other authors reported a general good performance of ACuZinc alloys, the alloys developed by General Motors to improve wear and creep resistance in zinc alloy family [51], as well as for Alzen alloys [31,46].

Finally, also cavitation erosion resistance of Zn-Al alloys was studied [67]. Interestingly, despite the higher hardness, it was found that high-Al alloys as such as ZA27 and Alzen 305 exhibited higher erosion rate than ZnAl15Cu1Mg alloy, as synthetized in Table 3. This was due to the positive role of eutectic β + η phase of the latter alloy, which was more resistant than primary phases. Therefore, since in ZA27 and Alzen 305 primary Al-rich phase is the most abundant, they were more damaged by cavitation erosion, as noticeable in Figure 8.

Table 3. Hardness and erosion rate according to ASTM G32 standard (based on data from [67]).

Alloy	HV Hardness	Erosion Rate (mm^3/h)
ZA27	164 ± 5	2.4
Alzen305	149 ± 13	1.9
ZnAl15Cu1Mg	122 ± 9	1.5

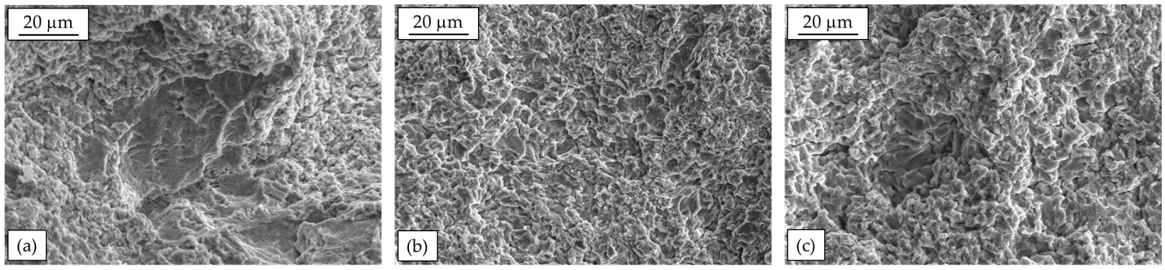

Figure 8. SEM analyses of the eroded surfaces after 8 hours for (**a**) ZA27, (**b**) ZnAl15Cu1Mg, and (**c**) Alzen305.

4.4. Creep

The mechanism of creep (time and temperature dependent deformation/plastic flow under a constant applied load) for Zn-Al alloys has been widely debated during the years. Indeed, because of their low melting points, this phenomenon is particularly relevant for this family of alloys and it is one of the reason for their limited applications for structural components, especially if exposed above 100 °C.

In general, three stages can be defined for the creep behavior of zinc alloys. The primary creep is dominated by strain hardening phenomena and is characterized by a decreasing in strain rate with time. During secondary creep, the strain rate is mainly constant since strain hardening effects are compensated by recovery phenomena. Finally, the tertiary creep, which leads to failure, sees a steep increase in strain rate due to a general softening of the matrix and reduction in the load bearing cross section.

Important parameters for designers are the time to set strain (e.g., time to 1% strain) and the stress to produce a set strain in a set time (e.g., stress needed to produce 0.2% strain in 100,000 h). Early studies on creep behavior of Zn-Al alloys allowed the identification of a relationship among creep elongation time, stress, and temperature by means of an empirical equation, that could be fit to the behavior of various Zn-Al alloys [68,69]. According to these findings, the creep elongation can be described by a simple empirical equation like

$$f(\varepsilon) = A\, t\, \sigma^n \exp(-Q/RT), \quad (1)$$

where A is a constant (function of alloy composition and structure), t is the time, σ is the nominal stress, n is the stress exponent, Q is the effective activation energy for creep, R is the gas constant, T is the absolute temperature of the test, and $f(\varepsilon)$ an undefined function of the creep strain ε.

The stress exponent n usually lies between 4 and 7 and it can be calculated experimentally from the power law function as the slope of the creep line (i.e., plotting the strain rate as a function of stress), while the activation energy Q can be determined performing the creep tests over a range of temperatures. For Zn alloys n is frequently found between 3.33 and 5 [40,68] while Q results about 94 kJ/mol for Zamak alloys and in the range 102–112 kJ/mol for ZA8, ZA12, and ZA27 [70,71]. A more detailed literature review about Q and n values for Zn alloys can be found in [71].

When A, σ, n, Q, and T are constant, this function corresponds to the creep strain versus time curve. Moreover, if $f(\varepsilon) = \varepsilon$, by differentiating both sides of the equation with respect to time, then Equation (1) corresponds to the power law representation for creep behavior in the steady state region [72].

Equation (1) can be further modified by using logarithms and rearranging it, as shown by Murphy et al. [73], to obtain

$$ln\ t = ln\ f(\varepsilon) - ln\ A - n\ (ln\ \sigma) + Q/RT, \quad (2)$$

and at a constant strain

$$ln\ t = C' - n\ (ln\ \sigma) + Q/RT, \quad (3)$$

where C' is a constant incorporating A and ε. Determination of the constant C' allows calculating, for instance, the design stresses able to produce 1% creep strain in 100,000 h at different temperatures.

Murphy et al. [73] developed creep curves and derived the values of the constant C' for Zamak 3, ZA-8, and ZA-27. This was later extended to Zamak 2 and 5 by Schrems et al. [74]. The values of C' for these alloys that can be used in Equation (3) for several levels of creep strain are shown in Table 4.

Table 4. Values of C′ for several alloys and levels of creep strain for use in Equation (3) (based on data from [40,73]).

Alloy	Strain Level			
	0.20%	**0.25%**	**0.50%**	**1.00%**
Zamak 2	-	−13.75	−12.65	−11.61
Zamak 3	−13.41	-	−11.86	−11.06
Zamak 5	-	−14.61	−13.56	−12.69
ZA-8	−10.90	-	−9.43	−8.43
ZA-27	−13.94	-	−11.91	−10.64

Various mechanisms have been discussed for creep deformation of Zn-Al alloys, ranging from dislocation-controlled creep to grain boundary sliding.

More in detail, considering hypoeutectic ZA8 alloy, the addition of Mn in order to enhance creep resistance was studied by [33]. It was found that the formation of Mn-containing intermetallic particles and their grain refining effect was beneficial for creep resistance of the alloy.

The role of primary creep was instead investigated for Zamak 5 as a function of aging time [75]. It was reported that the duration of the aging treatment affects the primary creep strain, while this does not happen for steady state creep, which is more related to other microstructural feature, as the aspect ratio of primary Zn particles.

Superplasticity of ZnAl22 eutectoid alloy has been also widely studied [76–79]. The addition of Cu is reported to improve creep resistance [80,81]. Interestingly, it was found that creep test at 150 °C are accompanied by a microstructural evolution of the alloy, involving the decomposition of the metastable phase η′, the four phase transformation, $\alpha + \varepsilon \sim T' + \eta$, and the development of the spheroidized structure from lamellar structure in the eutectoid Zn-Al based alloy. Such microstructural evolution plays a positive role for creep resistance of the material.

Regarding Zn-Cu alloys [82], it was found that Cu content of approximately 1 wt. % and aging treatment are positive for creep resistance, since they contribute to hinder grain boundary sliding during test. This has been exploited in the development of the ACuZinc alloys, which exhibit superior creep strength [83], and also several alloys near the Zn-Al-Cu ternary eutectic [84].

Coarser microstructures give higher creep resistance because of the lower density of grain boundaries. However, ultra-fine microstructures produced in 0.8 mm thick Zamak 5 die-castings show improved creep resistance [85].

4.5. Corrosion Resistance

Similarly to mechanical properties, also corrosion resistance of Zn alloys is linked to the microstructure, the chemical composition and the level of impurities. About the last, Pb, Sn, and Cd are known to cause intergranular corrosion in Zn-Al alloys and to reduce physical and mechanical

properties. For this reason, their level must be maintained within the limits specified in ASTM B86 standard and small amount of Mg is added to inhibit the phenomenon [5].

Concerning the main alloying elements, Cu has been found to have a beneficial effect on the atmospheric corrosion resistance. Also Al improves the corrosion resistance. In fact, the corrosion rate of the ZA alloys in water was demonstrated to increase below pH 6.0 and above pH 11.5, meanwhile for ZA27 it resulted one-third that of other Zn-Al alloys [8,86]. This because the corrosion attack appears mainly concentrated on the Zn-rich phase, whose amount is reduced by increasing the Al content. It is worth noting that for hypo-eutectic Zn-Al alloys, Ares et al. detected a decrease of corrosion resistance as the concentration of aluminum increases and that close to the eutectic composition this resistance depends on the microstructure [87].

Other authors investigated the role of the microstructure on corrosion behavior of Zn-Al alloys, analyzing the influence of coarse and fine columnar/equiaxed structures and of secondary dendrite arm spacing. Concerning the grain size of pure Zn, Osorio et al. demonstrated a better corrosion resistance of coarse structures than with fine grains in both columnar and equiaxed structures [88,89]. Moreover, for hypo-eutectic Zn-Al alloys, whose grain boundaries and inter-dendritic regions contain Al-rich phase in the lamellar eutectic mixture, it was found that a finer dendritic structure shows higher corrosion resistance than a coarser one. On the opposite, for hyper-eutectic Zn-Al alloys, coarser dendritic structures seem to improve the corrosion resistance because of the eutectoid decomposition [90].

Hence, it is general accepted that conventional Zn-Al alloys show good corrosion resistance in different environments and that their behavior is strongly affected by the solidification and cooling conditions (i.e., secondary dendrite arm spacing, grain size, and solute redistribution). However, many attempts have been performed to further improve this property by means of alternative alloy chemical compositions as such as Zn-Al alloys reinforced by different types of particles (zircon, graphite, fiber-glass, fly-ash, etc.) or with addition of Ag, Si, or rare earth elements.

For instance, Sharma et al. [91] investigated the corrosion performance of ZA27 reinforced ith zircon particles, finding that the corrosion rate in 1 N HCl decreases with the zircon content. The effect of graphite particle addition in ZA27 on corrosion resistance in 1 M HCl and in SAE 40 oil was studied by Seah et al. [92]. They showed that the composite corrodes in HCl, meanwhile in oil the corrosion resistance is enhanced. Also the addition of glass fibers to ZA27 resulted in an improvement of corrosion resistance [93]. Similar results were obtained by reinforcing ZA27 by fly-ash or Al_2O_3, what resulted was the improvement of resistance to uniform corrosion of the alloy [94].

Regarding the addition of alloying elements, tests performed on Zn-22 wt. % Al modified with silver showed that the corrosion behavior in saline solution is only weakly dependent on the Ag concentration [95]. On the contrary, the addition of REE appeared to improve the corrosion resistance of the ZnAl40Cu3 alloy, meanwhile that of Si seemed not to affect the behavior of the alloy [96].

Other papers dealing with corrosion resistance of modified Zn-Al alloys are available in the literature, however until now all these modification of standard Zn-Al alloys have not found real industrial applications.

5. Summary

In the present paper, an overview of the properties of Zn alloys is provided, paying particular attention to the identification of the correlation between microstructure and performance. In particular, after a first summary of commercial alloys and relative manufacturing processes, microstructural properties are described. In this regard, the discussion is focused on the Zn-Al and Zn-Cu systems, which are the most widely used. Subsequently, various aspects are described, as such as tensile properties, wear resistance, creep behavior, and corrosion resistance. A paragraph is also dedicated to the discussion of the effect of natural aging on material properties since Zn alloys are especially sensitive to this phenomenon. The general aim of the present discussion of properties of Zn-based alloy is to allow the reader to better understand the specific applications suitable for this family of alloys.

Author Contributions: Conceptualization, A.P.; analysis, A.P. and M.T.; writing—original draft preparation, A.P. and M.T.; writing—review, F.G.; editing A.P., M.T. and F.G. All authors have read and agreed to the published version of the manuscript.

Funding: This research received no external funding.

Acknowledgments: The authors would like to thank Didier Rollez and Lorenzo Montesano for the precious support.

Conflicts of Interest: The authors declare no conflict of interest.

References

1. Global Zinc Market to Grow at 3.8% in 2022. Available online: https://www.mining-technology.com/comment/zinc-outlook-2019/ (accessed on 5 January 2020).
2. Lynch, R.F. Zinc: Alloying, Thermomechanical Processing, Properties, and Applications. In *Encyclopedia of Materials: Science and Technology*; Elsevier: Amsterdam, The Netherland, 2001; pp. 9869–9883.
3. Marder, A.R. Metallurgy of zinc-coated steel. *Prog. Mater. Sci.* **2000**, *45*, 191–271. [CrossRef]
4. Levy, G.K.; Goldman, J.; Aghion, E. The prospects of zinc as a structural material for biodegradable implants: A review paper. *Metals* **2017**, *7*, 402. [CrossRef]
5. Rollez, D.; Pola, A.; Prenger, F. Zinc alloy family for foundry purposes. *World Metall.* **2015**, *68*, 354–358.
6. The New Generation of Efficient and Sustainable Zinc Alloys. Available online: https://grillo.de/wp-content/uploads/2014/08/grillo_flyer_zep_englisch_v2_141019.pdf (accessed on 5 January 2020).
7. Goodwin, F.E. Zinc and Zinc alloys. In *Marks' Standard Handbook for Mechanical Engineers*, 12th ed.; Sadegh, A.M., Worek, W.M., Eds.; McGraw-Hill Education: New York, NY, USA, 2018.
8. Kubel, E.J., Jr. Expanding horizon for ZA alloys. *Adv. Mater.Process.* **1987**, *132*, 51–57.
9. Prasad, B.K.; Patwardhan, A.K.; Yegneswaran, A.H. Dry sliding wear characteristics of some zinc-aluminium alloys: A comparative study with a conventional bearing bronze at a slow speed. *Wear* **1996**, *199*, 142–151. [CrossRef]
10. Abou El-Khair, M.T.; Daoud, A.; Ismail, A. Effect of different Al contents on the microstructure, tensile and wear properties of Zn-based alloy. *Mater. Lett.* **2004**, *58*, 1754–1760. [CrossRef]
11. Porter, F. *Zinc handbook: Properties, Processing, and Use In Design*; CRC Press: New York, NY, USA, 1991.
12. Gervais, E.; Barnhurst, R.J.; Loong, C.A. An Analysis of Selected Properties of ZA Alloys. *JOM* **1985**, *37*, 43–47. [CrossRef]
13. *ASTM-B86-13 Standard Specification for Zinc and Zinc-Aluminum (ZA) Alloy Foundry and Die Castings*; ASTM International: West Conshohocken, PA, USA, 2013.
14. Ross, R.B. Zinc. In *Metallic Materials Specification Handbook*; Springer: New York, NY, USA, 1992; pp. 614–617.
15. Cho, T.-S.; Lee, H.-J.; Ahn, B.; Kawasaki, M.; Langdon, T.G. Microstructural evolution and mechanical properties in a Zn-Al eutectoid alloy processed by high-pressure torsion. *Acta Mater.* **2014**, *72*, 67–79. [CrossRef]
16. Zhu, Y.H.; Lee, W.B.; To, S. Ageing characteristics of cast Zn-Al based alloy ($ZnAl_7Cu_3$). *J. Mater. Sci.* **2003**, *38*, 1945–1952. [CrossRef]
17. Apelian, D.; Paliwal, M.; Herrschaft, D.C. Casting with zinc alloys. *JOM* **1981**, *33*, 12–20. [CrossRef]
18. Kapranos, P.; Brabazon, D.; Midson, S.P.; Naher, S.; Haga, T. Advanced Casting Methodologies: Inert Environment Vacuum Casting and Solidification, Die Casting, Compocasting, and Roll Casting. In *Comprehensive Materials Processing*; Elsevier: Amsterdam, The Netherlands, 2014; pp. 3–37.
19. Cooper, D.R.; Rossie, K.E.; Gutowski, T.G. An environmental and cost analysis of stamping sheet metal parts. *J. Manuf. Sci. Eng.* **2017**, *139*, 041012. [CrossRef]
20. Barnhurst, R.J. Zinc and Zinc Alloys. In *Properties and Selection: Nonferrous Alloys and Special-Purpose Materials*; ASM International: Materials Park, OH, USA, 1990; pp. 1619–1653.
21. Savaşkan, T.; Hekimoğlu, A.P. Microstructure and mechanical properties of Zn-15Al-based ternary and quaternary alloys. *Mater. Sci. Eng. A* **2014**, *603*, 52–57. [CrossRef]
22. Rollez, D.; Pola, A.; Montesano, L.; Brisitto, M.; De Felicis, D.; Gelfi, M. Effect of aging on microstructure and mechanical properties of ZnAl15Cu1 alloy for wrought applications. *Int. J. Mater. Res.* **2017**, *108*, 447–454. [CrossRef]
23. To, S.; Zhu, Y.H.; Lee, W.B. Use of EBSD to identify phases in interdendrite region of a cast Zn–Al-based alloy (ZA27). *J. Microsc.* **2007**, *225*, 170–174. [CrossRef]

24. Campbell, J. *The New Metallurgy of Cast Metals Castings*; Butterworth-Heinemann: Oxford, UK, 2003.
25. ACuzinc. Available online: http://www.brockmetals.sk/product_acuzinc.html (accessed on 5 January 2020).
26. ACuzinc 5. Available online: https://www.dynacast.com/acuzinc5 (accessed on 10 January 2020).
27. Nevison, D.C.H. Zinc and Zinc Alloys. In *ASM Handbook Volume 15: Casting*; ASM International: Materials Park, OH, USA, 2008; pp. 1735–1755.
28. Liu, Z.; Li, R.; Jiang, R.; Li, X.; Zhang, M. Effects of Al addition on the structure and mechanical properties of Zn alloys. *J. Alloys Compd.* **2016**, *687*, 885–892. [CrossRef]
29. Hekimoğlu, A.P.; Savaşkan, T. Structure and mechanical properties of Zn-(5–25) Al alloys. *Int. J. Mater. Res.* **2014**, *105*, 1084–1089. [CrossRef]
30. Pola, A.; Montesano, L.; Roberti, R. Nuove Leghe di Zinco per L'industria del Design. In Proceedings of the 30th Convegno Nazionale AIM, Brescia, Italy, 10–12 November 2010.
31. Savaşkan, T.; Hekimoglu, A.P.; Pürçek, G. Effect of copper content on the mechanical and sliding wear properties of monotectoid-based zinc-aluminium-copper alloys. *Tribol. Int.* **2004**, *37*, 45–50. [CrossRef]
32. Luo, X.-P.; Xia, L.-T.; Zhang, M.-G. Effect of different Al content on the microstructure, mechanical and friction properties of high aluminum zinc-based alloys. *J. Adv. Microsc. Res.* **2011**, *6*, 301–305. [CrossRef]
33. Türk, A.; Durman, M.; Kayali, E.S. The effect of manganese on the microstructure and mechanical properties of zinc–aluminium based ZA-8 alloy. *J. Mater. Sci.* **2007**, *42*, 8298–8305. [CrossRef]
34. Li, M.; Lu, S.; Long, F.; Sheng, M.; Geng, H.; Liu, W. Effect of Y Addition on the Mechanical Properties and Microstructure of Zn-Al Alloys. *JOM* **2015**, *67*, 922–928. [CrossRef]
35. Gancarz, T.; Cempura, G. Characterization of ZnAl cast alloys with Li addition. *Mater. Des.* **2016**, *104*, 51–59. [CrossRef]
36. Krupińska, B. Structure and Properties of Zn–Al–Cu Alloys with Alloying Additives. *Adv. Struct. Mater.* **2015**, *70*, 341–349. [CrossRef]
37. Choudhury, P.; Das, K.; Das, S. Evolution of as-cast and heat-treated microstructure of a commercial bearing alloy. *Mater. Sci. Eng. A* **2005**, *398*, 332–343. [CrossRef]
38. Savaşkan, T.; Bican, O. Effects of silicon content on the microstructural features and mechanical and sliding wear properties of Zn–40Al–2Cu–(0–5)Si alloys. *Mater. Sci. Eng. A* **2005**, *404*, 259–269. [CrossRef]
39. Pola, A.; Gelfi, M.; La Vecchia, G.M.; Montesano, L. On the ageing of a hyper-eutectic Zn-Al alloy. *Metall. Ital.* **2015**, *107*, 37–41.
40. Goodwin, F.E.; Kallien, L. Improving the Relationship between Processing and Properties of Zinc Die Casting: Developments in Creep and Ageing Correlations. *SAE Int. J. Mater. Manuf.* **2011**, *4*, 1188–1197. [CrossRef]
41. Kallien, L.H.; Leis, W. Ageing of Zink Alloys. *Int. Foundry Res.* **2011**, *64*, 2–23.
42. Leis, W.; Kallien, L. Ageing and creep of Zinc-Diecast. In Proceedings of the International Zinc Diecasting Conference 2013, Praha, Czech Republic, 13–14 June 2013.
43. Dorantes-Rosales, H.J.; López-Hirata, V.M.; Hernández-Santiago, F.; Saucedo-Muñoz, M.L.; Paniagua-Mercado, A.M. Effect of Ag addition to Zn22 mass%Al2 mass%Cu alloy on the four-phase reaction. *Mater. Trans.* **2018**, *59*, 717–723. [CrossRef]
44. Chen, Y.; Tu, M. Dimensional shrinkage of supersaturated ZA27Cu1 and ZA27Cu2 alloys. *Mater. Sci. Techol.* **1998**, *14*, 473–475. [CrossRef]
45. Chen, H.; Xin, X.; Dong, D.Y.; Ren, Y.P.; Hao, S.M. Study on the stability of T′ phase in the Al-Zn-Cu ternary system. *Acta Metall. Sinca* **2004**, *17*, 269–273.
46. Lee, P.P.; Savaskan, T.; Laufer, E. Wear resistance and microstructure of Zn-Al-Si ans Zn-Al-Cu alloys. *Wear* **1987**, *117*, 79–89. [CrossRef]
47. Türk, A.; Kurnaz, C.; Şevik, H. Comparison of the wear properties of modified ZA-8 alloys and conventional bearing bronze. *Mater. Des.* **2007**, *28*, 1889–1897. [CrossRef]
48. Savaşkan, T.; Maleki, R.A. Friction and wear properties of Zn-25Al-based bearing alloys. *Tribol. Trans.* **2014**, *57*, 435–444. [CrossRef]
49. Babic, M.; Mitrovic, S.; Jeremic, B. The influence of heat treatment on the sliding wear behavior of a ZA-27 alloy. *Tribol. Int.* **2010**, *43*, 16–21. [CrossRef]
50. Pürçek, G.; Savaskan, T.; Küçükömeroglu, T.; Murphy, S. Dry sliding friction and wear properties of zinc-based alloys. *Wear* **2002**, *252*, 894–901. [CrossRef]
51. Hanna, M.D.; Carter, J.T.; Rashid, M.S. Sliding wear and friction characteristics of six Zn-based die-casting alloys. *Wear* **1997**, *203–204*, 11–21. [CrossRef]

52. Pola, A.; Montesano, L.; Gelfi, M.; La Vecchia, G.M. Comparison of the sliding wear of a novel Zn alloy with that of two commercial Zn alloys against bearing steel and leaded brass. *Wear* **2016**, *368–369*, 445–452. [CrossRef]
53. Şevic, H. The effect of silver on wear behaviour of zinc–aluminium-based ZA-12 alloy produced by gravity casting. *Mater. Charact.* **2010**, *89*, 81–87. [CrossRef]
54. Çuvalcı, H.; Çelik, H.S. Investigation of the abrasive wear behaviour of ZA-27 alloy and CuSn10 bronze. *J. Mater. Sci.* **2011**, *46*, 4850–4857. [CrossRef]
55. Miroslav, B.; Vencl, A.; Mitrović, S.; Bobić, I. Influence of T4 heat treatment on tribological behavior of Za27 alloy under lubricated sliding condition. *Tribol. Lett.* **2009**, *36*, 125–134. [CrossRef]
56. Li, Y.; Ngai, T.L.; Xia, W.; Zhang, W. Effects of Mn content on the tribological behaviors of Zn-27% Al-2% Cu alloy. *Wear* **1996**, *198*, 129–135. [CrossRef]
57. Haroan, G.; Jiaji, M. Alloying of Zn-27% Al with antimony. *Int. J. Cast Metal. Res.* **1999**, *11*, 205–210. [CrossRef]
58. Murphy, S.; Savaşkan, T. Comparative wear behavior of Zn-Al-based alloys in automotive engine application. *Wear* **1984**, *98*, 151–161. [CrossRef]
59. Çuvalcı, H.; Bas, H. Investigation of the tribological properties of silicon containing zinc–aluminum based journal bearings. *Tribol. Int.* **2004**, *37*, 433–440. [CrossRef]
60. Babić, M.; Mitrović, S.; Ninković, R. Tribological Potencial of Zinc-Aluminium Alloys Improvement. *Tribol. Ind.* **2009**, *31*, 15–28.
61. Miroslav, B.; Mitrović, S.; Zivic, F.; Bobić, I. Wear behavior of composites based on ZA-27 alloy reinforced by Al2O3 particles under dry sliding condition. *Tribol. Lett.* **2010**, *38*, 337–346. [CrossRef]
62. Sharma, S.C.; Krishna, M.; Bhattacharyya, D. Dry sliding wear behaviour of flyash reinforced ZA-27 alloy based metal matrix composites. *Int. J. Mod. Phys. B* **2006**, *20*, 4703–4708. [CrossRef]
63. Sharma, S.C.; Girish, B.M.; Somashekar, D.R.; Satish, B.M.; Kamath, R. Sliding wear behaviour of zircon particles reinforced ZA-27 alloy composite materials. *Wear* **1999**, *224*, 89–94. [CrossRef]
64. Yan, S.; Xie, J.; Liu, Z.; Wang, W.; Wang, A.; Li, J. Influence of different Al contents on microstructure, tensile and wear properties of Zn-based alloy. *J. Mater. Sci. Technol.* **2010**, *26*, 648–652. [CrossRef]
65. Yan, S.; Xie, J.; Liu, Z.; Li, J.; Wang, W.; Wang, A. The effect of composition segregation on the friction and wear properties of ZA48 alloy in dry sliding condition. *J. Mater. Sci.* **2009**, *44*, 4169–4173. [CrossRef]
66. Savaşkan, T.; Pürçek, G.; Hekimoğlu, A.P. Effect of Copper content on the mechanical and tribological properties of ZnAl27-based alloys. *Tribol. Lett.* **2003**, *15*, 257–263. [CrossRef]
67. Montesano, L.; Pola, A.; La Vecchia, G.M. Cavitation-erosion resistance of three zinc-aluminum alloy for bearing application. *Metall. Ital.* **2016**, *11*, 50–55.
68. Murphy, S.; Savaskan, T.; Hill, J. The creep kinetics of zinc-aluminium-based alloys. *Can. Metall. Q.* **1986**, *25*, 145–150. [CrossRef]
69. Savaskan, T.; Murphy, S. Creep behavior of Zn-Al-Cu alloys. *Z. Metallkd.* **1983**, *74*, 76–82.
70. Anwar, M.; Murphy, S. Creep kinetics in compression of sand cast commercial Zn-Al alloys. *Mater. Sci. Technol.* **2000**, *16*, 321–332. [CrossRef]
71. Wu, Z.; Sandlöbes, S.; Wang, Y.; Gibson, J.S.K.-L.; Korte-Kerzel, S. Creep behaviour of eutectic Zn-Al-Cu-Mg alloys. *Mater. Sci. Eng. A* **2018**, *724*, 80–94. [CrossRef]
72. Evans, R.W.; Wildshire, B. *Introduction to Creep*; The Institute of Materials: London, UK, 1983.
73. Murphy, S.; Durman, M.; Hill, J. Kinetics of creep in pressure diecast commercial Zinc-Aluminium alloys. *Z. Metallkd.* **1988**, *79*, 243–247.
74. Schrems, K.K.; Dogan, O.N.; Goodwin, F.E. Creep Properties of Die Cast Zinc Alloys. In Proceedings of the NADCA CastExpo 2010, Orlando, FL, USA, 20–23 March 2010.
75. Roberti, R.; Pola, A.; Gilles, M.; Rollez, D. Primary and steady state creep deformation in Zamak5 die-casting alloy at 80 °C. *Mater. Charact.* **2008**, *59*, 1747–1752. [CrossRef]
76. Mishra, R.S.; Murty, G.S. The stress-strain rate behaviour of superplastic Zn-Al eutectoid alloy. *J. Mater. Sci.* **1988**, *23*, 593–597. [CrossRef]
77. Xia, S.H.; Wang, J.; Wang, J.T.; Liu, J.Q. Improvement of room-temperature superplasticity in Zn–22 wt. %Al alloy. *Mater. Sci. Eng. A* **2008**, *493*, 111–115. [CrossRef]
78. Huang, Y.; Langdon, T.G. Characterization of deformation processes in a Zn-22% Al alloy using atomic force microscopy. *J. Mater. Sci.* **2002**, *37*, 4993–4998. [CrossRef]

79. Demirtas, M.; Kawasaki, M.; Yanar, H.; Purcek, G. High temperature superplasticity and deformation behavior of naturally aged Zn-Al alloys with different phase compositions. *Mater. Sci. Eng. A* **2018**, *730*, 73–83. [CrossRef]
80. Zhu, Y.H. Creep induced phase transformation in cast Zn-Al alloy. *J. Mater. Sci. Lett.* **1996**, *15*, 1358–1360. [CrossRef]
81. Zhu, Y.H. Microstructure dependence of the creep behavior of a Zn–Al based alloy. *J. Mater. Process. Technol.* **1998**, *73*, 18–24. [CrossRef]
82. Sharma, R.C.; Martin, J.W. Creep of dilute zinc-copper alloys. *J. Mater. Sci.* **1974**, *9*, 1139–1144. [CrossRef]
83. Rashid, X.M.S.; Hanna, M.D. ACuZinc: Improved Zinc Alloys for Die Casting Applications. *SAE Tech. Pap.* **1993**. [CrossRef]
84. Winter, R.E. EZAC™—A novel high strength, creep resistant, hot chamber zinc die casting alloy. *SAE Tech. Pap.* **2011**. [CrossRef]
85. Frank, T.; Kansy, A.; Kallien, L.; Leis, W.; Goodwin, F.E. Effect of Zinc Alloy Casting Section Thickness on Creep Behavior. In Proceedings of the NADCA 2019 Die Casting Congress and Tabletop, Paper T19-102, Cleveland, OH, USA, 2 October 2019.
86. Choudhury, P.; Das, S. Effect of microstructure on the corrosion behavior of a zinc-aluminium alloy. *J. Mater. Sci.* **2005**, *40*, 805–807. [CrossRef]
87. Ares, A.E.; Gassa, L.M.; Schvezov, C.E.; Rosenberger, M.R. Corrosion and wear resistance of hypoeutectic Zn-Al alloys as a function of structural features. *Mater. Chem. Phys.* **2012**, *136*, 394–414. [CrossRef]
88. Osório, W.R.; Freire, C.M.; Garcia, A. The role of macrostructural morphology and grain size on the corrosion resistance of Zn and Al castings. *Mater. Sci. Eng. A* **2005**, *402*, 22–23. [CrossRef]
89. Osório, W.R.; Spinelli, J.E.; Freire, C.M.; Garcia, A. The role of macrostructural and microstructural morphologies on the corrosion resistance of Zn and a Zn-4% Al alloy. *Mater. Manuf. Process.* **2007**, *22*, 341–345. [CrossRef]
90. Osório, W.R.; Freire, C.M.; Garcia, A. The effect of the dendritic microstructure on the corrosion resistance of Zn-Al alloys. *J. Alloys Compd.* **2005**, *397*, 179–191. [CrossRef]
91. Sharma, S.C.; Somashekar, D.R.; Satish, B.M. A note on the corrosion characterisation of ZA-27/zircon particulate composites in acidic medium. *J. Mater. Process. Technol.* **2011**, *118*, 62–64. [CrossRef]
92. Seah, K.H.W.; Sharma, S.C.; Girish, B.M. Corrosion characteristics of ZA-27-graphite particulate composites. *Corros. Sci.* **1997**, *39*, 1–7. [CrossRef]
93. Sharma, S.C.; Seah, K.H.W.; Satish, B.M.; Girish, B.M. Corrosion characteristics of ZA-27/glass-fibre composites. *Corros. Sci.* **1997**, *39*, 2143–2150. [CrossRef]
94. Almomani, M.; Hayajneh, M.T.; Draidi, M. Corrosion investigation of zinc-aluminum alloy matrix (ZA-27) reinforced with alumina (Al_2O_3) and fly ash. *Particul. Sci. Technol.* **2017**, *35*, 439–447. [CrossRef]
95. Flores, M.; Huerta, L.; Casolco, S.R.; Muhl, S.; Torres-Villaseñor, G.; Luna, J.A. The Effect of Ag addition on the corrosion of Zn-22wt. %Al Alloys. In Proceedings of the Materials Research Society Symposium Proceedings, San Francisco, CA, USA, 22–25 April 2003; pp. 65–70.
96. Michalik, R. Influence of Si and REE on the corrosion resistance of ZnAl40Cu3 alloy. *Solid State Phenom.* **2014**, *212*, 133–136. [CrossRef]